CrossMark

Severe Autumn storms in future Western Europe with a warmer Atlantic Ocean

**Michiel Baatsen · Reindert J. Haarsma ·
Aarnout J. Van Delden · Hylke de Vries**

Abstract Simulations with a very high resolution (~25 km) global climate model indicate that more severe Autumn storms will impact Europe in a warmer future climate. The observed increase is mainly attributed to storms with a tropical origin, especially in the later part of the twentyfirst century. As their genesis region expands, tropical cyclones become more intense and their chances of reaching Europe increase. This paper investigates the properties and evolution of such storms and clarifies the future changes. The studied tropical cyclones feature a typical evolution of tropical development, extratropical transition and a re-intensification. A reduction of the transit area between regions of tropical and extratropical cyclogenesis increases the probability of re-intensification. Many of the modelled storms exhibit hybrid properties in a considerable part of their life cycle during which they exhibit the hazards of both tropical and extratropical systems. In addition to tropical cyclones, other systems such as cold core extratropical storms mainly originating over the Gulf Stream region also increasingly impact Western Europe. Despite their different history, all of the studied storms have one striking similarity: they form a warm seclusion. The structure, intensity and frequency of storms in the present climate are compared to observations using the MERRA and IBTrACS datasets. Damaging winds associated with the occurrence of a sting jet are observed in a large fraction of the cyclones during their final stage. Baroclinic instability is of great importance for the (re-)intensification of the storms. Furthermore, so-called atmospheric rivers providing tropical air prove to be vital for the intensification through diabatic heating and will increase considerably in strength in the future, as will the associated flooding risks.

List of symbols

DT	EPT difference between the core and the minimum in the south–east quadrant of a storm
$DT_{850,max}$	Maximum EPT difference in a cyclone at 850 hPa
EPT	Equivalent potential temperature
ETC	Extratropical cyclone
ETT	Extratropical transition
IVT	Integrated vapour transport
MSLP	Mean sea level pressure
P_{min}	Minimum MSLP of a cyclone
PT	Potential temperature
PTC	Post-tropical cyclone
PV	Potential vorticity
PVU	Potential vorticity units (10^{-6} Km^2/kgs)
Q_c	Total amount of core moisture in a cyclone
RV	Relative vorticity
SST	Sea surface temperature
TC	Tropical cyclone
$V_{10,max}$	Maximum 10 m wind speed found within 20 grid boxes of a storm's centre
Z_d	Storm relative thickness asymmetry of 850–300 hPa layer

M. Baatsen · R. J. Haarsma · H. de Vries
Royal Netherlands Meteorological Institute (KNMI), De Bilt, The Netherlands

M. Baatsen (✉) · A. J. Van Delden
Institute for Marine and Atmospheric Research, Utrecht University, Heidelberglaan 8, 3584 CS Utrecht, The Netherlands
e-mail: m.l.j.baatsen@uu.nl

Springer

1 Introduction

Severe wind storms in Western Europe can cause major damage in coastal regions (Dorland et al. 1999). As their impacts are likely to increase in the future (Schwierz et al. 2009), it is important to assess changes in intensity and frequency of such storms. In the present climate most of the intense storms occur in winter, but a recent study (Haarsma et al. 2013) predicts some major changes by the end of the twentyfirst century. For the future climate, a significant increase in storminess is to be expected during Autumn in Western Europe, due to a shift in the storm genesis region.

Haarsma et al. (2013) used a very high resolution global climate model (~25 km) that is capable of resolving tropical cyclones explicitly. They showed that the number of Beaufort 12 (>32.6 m/s) storms impacting Europe increases considerably in future climate simulations. Mainly the eastward expansion of the tropical cyclone genesis is thought to be responsible for storms forming further east and recurving towards Europe. Because of their origin, these systems are thought to be tropical cyclones undergoing extratropical transition and eventually re-intensifying as an extratropical cyclone. Only a limited set of storms was considered and the statistical analysis was limited to certain wind speed events. For this paper, a more extensive set of storms is selected (including Beaufort 11) of which the evolution is studied in greater detail. A case study was considered in Haarsma et al. (2013), which is discussed more elaborately. The aim is to identify the processes that determine the life cycle of storms impacting Europe, assess their impacts and predict related future changes. Storms in the near future (2030 s) are now also considered as an indication for the homogeneity and consistency of changes throughout the twentyfirst century.

In what follows, a case study of one specific storm is considered, sharing some characteristics with Hurricane Sandy (2012) and serving as an example of intense storms impacting Europe in future simulations. Section 3 provides information about the model data, selection and tracking procedures as well as the basics of the analysis techniques. In Sect. 4 the results of those analyses are presented, studying the properties of storms throughout their life cycles. Next, the mean appearance of all storms is investigated and compared to that of a warm seclusion cyclone. Finally, the intensification process is studied in more detail to identify the most important mechanisms. The general findings are then discussed and the paper is concluded in Sect. 5.

2 Case study: Amy

An intense storm developing in future simulations, hence called "Amy" for easy reference, is studied extensively as it shows many of the characteristics shared by other intense storms impacting Europe. In the first stage of its life-cycle (Fig. 1a, d), the storm is a mature tropical cyclone (TC; a list of acronyms is provided above) with high wind speeds in a confined area, a warm core and a narrow upright column of high potential vorticity (PV). The equivalent potential temperature (EPT) fields indicate that the cyclone carries a lot of warm and moist air from the tropics. A few days later, the storm enters the mid-latitudes with cooler sea surface temperatures (SSTs) and strong vertical wind shear (Fig. 1b). The system develops frontal characteristics with a distinct warm front forming to the north. A mid-latitude trough approaches from the west (indicated by the jet stream pattern), providing baroclinic instability. In fact, a cold-core cyclone is already forming just north of Amy. The dry intrusion (indicated by high PV) and jet stream presence can be seen in the according vertical cross section (Fig. 1e). At this point, the PV column is degrading at the top and the wind field is expanding which is consistent with the process of extratropical transition (ETT, Jones et al. 2003). Moreover, the PV column is tilting north-westward with height (towards the trough), indicative for rapid baroclinic development (Hoskins et al. 1977). At the same time, an atmospheric river (Zhu and Newell 1998) carrying high EPT tropical air to the mid-latitudes is present to the south–west of the storm. When Amy eventually merges with the other cyclone, all the ingredients for rapid cyclogenesis are present (left exit region of a jet streak, tilt of the PV column and strong EPT gradients). Consequently, the former tropical cyclone re-intensifies into a large and extremely powerful extra-tropical storm (Fig. 1c, f). The central pressure falls below 940 hPa and 3 hourly 850 hPa wind speeds exceed 50 m/s. A new dry intrusion is now located south of the centre and the remaining PV core has become vertically stacked (Fig. 1f), marking the end of baroclinic development in a mature extratropical cyclone (Hoskins 1990).

The structure of Amy differs from that of cyclones which are typically observed in Western Europe, as described by the Norwegian conceptual model (Bjerknes 1919; Bjerknes and Solberg 1922). The storm features a strong elongated warm front and a region of warmer air that is separated from the warm sector by cold air. This resembles the final stage of the Shapiro–Keyser conceptual model (Shapiro and Keyser 1990) and is known as a warm seclusion. Numerical simulations in the early 1990s pointed out that the evolution of extratropical cyclones is governed by the large scale background flow (Hoskins 1990; Davies et al. 1991; Thorncroft et al. 1993). Two extremes were discussed by Thorncroft et al. (1993) and called LC1 and LC2 cyclones, showing some resemblance with the Shapiro–Keyser and Norwegian conceptual model, respectively. LC1 type cyclones are typically observed at the storm track entrance region (confluent flow e.g. US East Coast) while
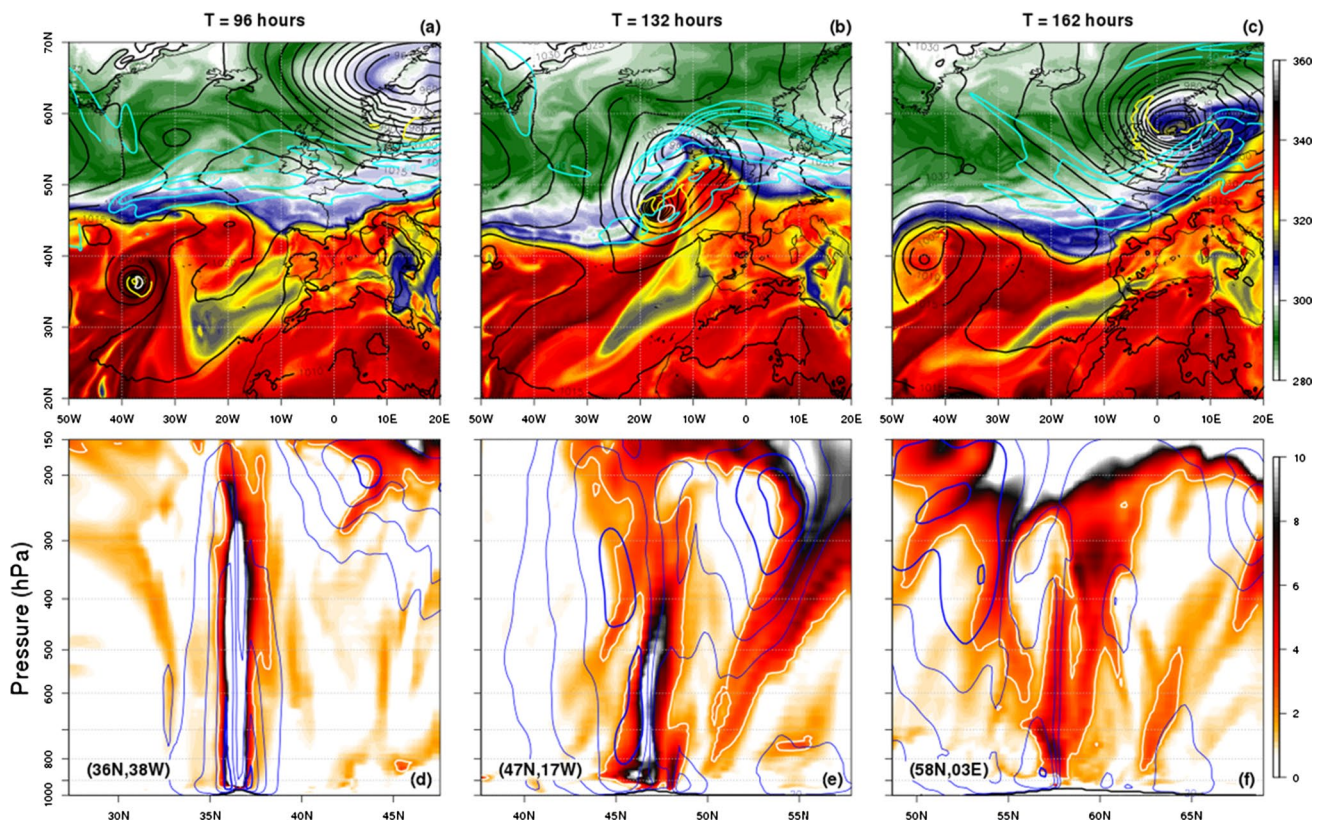
Fig. 1 Horizontal (**a–c**) and vertical (**d–f**) fields for Amy at 3 different stages; TC (*left*), extratropical transition (*middle*) and re-intensification (*right*). In the *upper panels*, *shading* represents 850 hPa EPT (K), *black contours* are mean sea level pressure (hPa), *cyan* indicates 250 hPa wind speed starting at 40 m/s with 10 m/s intervals and the *yellow* and *white contour* depict 33 and 50 m/s wind speed at 850 hPa. The *lower panels* contain PV (PVU) in *shading* and *contours* of horizontal wind speed (*thin lines* indicate 20, 30 and 40 m/s, *thick lines* 50 and 60 m/s). At the *bottom left*, the location of the storm centre at the respective times

the LC2 type ones usually occur at the exit region (diffluent flow e.g. Western Europe). This picture was found to be too simple and has been expanded and nuanced by Schultz et al. (1998) but still serves as a good baseline to distinguish different types of extratropical cyclones. Warm seclusion cyclones usually form as cold core systems but in the case of Amy, the remnant warm core of a TC is incorporated into the warm sector. During the fast development, a dry intrusion wraps around the tip of the warm conveyor belt forming a shallow warm core. Both baroclinic forcing and diabatic heating aid the intensification of extratropical cyclones exhibiting a warm core (van Delden 1989; Wernli et al. 2002), which are among the strongest observed on Earth (Maue 2010).

In the case of Amy, the presence of a shallow warm core is indeed suggested by both the EPT (Fig. 1c) and the decreasing wind speed with height near the centre (Fig. 1f). Related to warm seclusion storms is the possible presence of a sting jet, which can cause significant damage (Baker 2009). The occurrence of a sting jet in Amy is visible through the presence of a secondary wind maximum, located south–east of the storm centre at the end of

the back bent front (Fig. 1c). This region lies beneath the jet stream, of which the momentum can be transported downward by vertical motion leading to very strong winds near the surface. The corresponding vertical cross sections (Fig. 2) show an area of high wind speeds coming down from the jet and approaching the surface. This happens just south (Fig. 2a) and east (Fig. 2b) of the warm core and thus next to the back bent front. The pattern looks very similar to that shown in Figs. 5.12 and 5.13 of Maue (2010), apart from the absence of a strong wind field along the cold front. Additional figures showing the thermal evolution (Fig. S1) and precipitation (Fig. S2) associated with Amy can be found in the supplemental material.

The structure and evolution of Amy show some striking similarities with those of Hurricane Sandy in 2012 (such as size, structure and intensity). The latter also possessed the characteristics of a warm seclusion during its final stage of development (Galarneau et al. 2013). As this storm had an enormous socio-economic impact on a well-developed region, it is important to assess whether similar systems could hit Western Europe in the future. The question then remains whether the development of Amy is indicative for
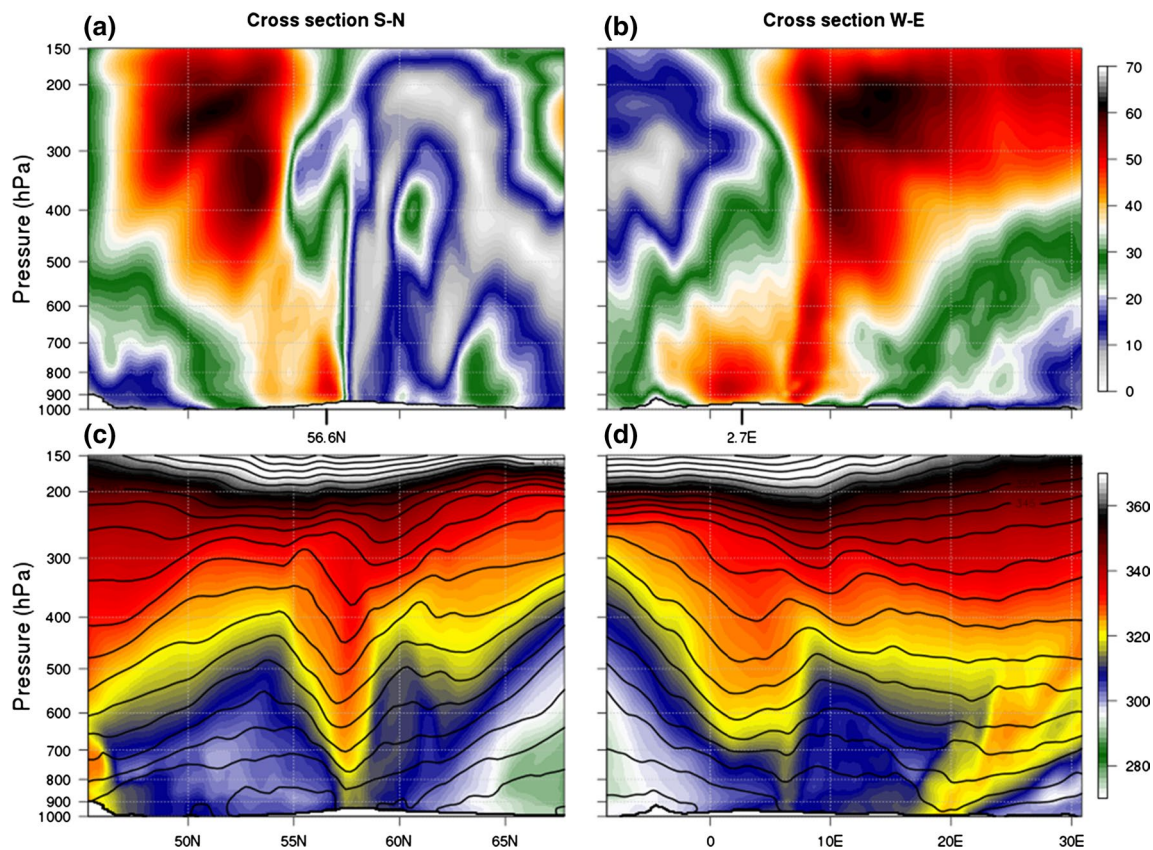
Fig. 2 Vertical cross sections of horizontal wind speed (m/s; **a**, **b**) and EPT (K; **c**, **d**) at t = 162 h. Both cross sections are taken 1.25° south of the MSLP minimum. The horizontal coordinates of the cross section are given in the axes of (**a**) and (**b**)

other future storms simulated by EC-Earth. In the present climate TCs do occasionally reach the mid-latitudes and re-intensify into powerful storms such as hurricane Irene in 1999 (Agusti-Panareda et al. 2004). Although relatively rare, warm seclusion cyclones are being observed in Western Europe, for example the Great Storm of 1987 (Browning 2004). It should be tested whether these storms are more common among the most intense Autumn storms in both observations and simulations, and whether this will change in the future.

3 Model characteristics and methodology

3.1 Model specifications

Simulations were done using the EC-Earth v2.3 model (Hazeleger et al. 2010) at a resolution of T799 L91 (~25 km), which was the operational resolution at the European Centre for Medium Range Weather Forecasts (ECMWF) from February 2006 until January 2010. Different model runs were performed for the present (2002–2006), near future (2030–2034) and future (2094–2098)

climate. Each of these datasets consists of a 6-member ensemble spanning 5 years resulting in a 30 year dataset. In present simulations, observed greenhouse gas and aerosol concentrations were applied while near future and future concentrations were derived from the RCP 4.5 scenario (van Vuuren et al. 2011). Only the atmosphere and land surface (HTESSEL; van den Hurk et al. 2000) are solved explicitly by the model to allow for the generation of high resolution results spanning an extensive period of time. Therefore, SST were imposed using daily data at 0.25° resolution from NASA (http://www.ncdc.noaa.gov/oa/climate/research/sst/oi-daily.php) for the 2002-2006 period. An estimate of the SST for the other periods was made by adding the ensemble mean predicted change using ECHAM5/MPI-OM in the ESSENCE project (Sterl et al. 2008) which used the SRES A1B scenario. This is comparable to RCP 4.5 scenario, having a slightly smaller global temperature increase by the end of the twentyfirst century (Rogelj et al. 2012). Some further details on model set-up and spin-up procedures can be found in Haarsma et al. (2013). The generated data is stored on 5 pressure levels (850, 700, 500, 300 and 200 hPa) at 6-hourly intervals, surface fields are saved 3 hourly. Only in the case of Amy, the

results on all model levels are saved at the same temporal resolution.

3.2 Observations

Although there are some shortcomings when using an atmospheric model with imposed SSTs, the high resolution allows for a first assessment of the influence of TCs in a global future climate perspective. As was demonstrated by the case study, both tropical and extratropical weather systems are well reproduced by the model. Yet, it is still of great importance to validate the results with observational data. This is done using the NCEP MERRA dataset (http://disc.sci.gsfc.nasa.gov/daac-bin/DataHoldings.pl). The 1981–2010 period is considered, based on 6-hourly assimilated data at a 0.5° by 0.67° horizontal resolution (lat, lon) and 42 vertical levels, serving as a reference for the 2002–2006 period. As the resolution of the reanalysis is still too coarse to accurately represent tropical cyclones, the IBTrACS database (http://www.ncdc.noaa.gov/ibtracs) is used to compare 1981–2010 tropical cyclone tracks reaching Europe to those generated by the model. A 30 year period is considered as the frequency of the studied storms is low and for better comparison with the total time span of present climate simulations.

3.3 Storm selection and tracking

For each period, a selection of storms is made using several selection criteria. To start with, cases where the (3-hourly) 10 m wind speed exceeds Beaufort 11 (28.4 m/s) are considered as severe storms. This is done for 4 different regions: Gulf of Biscay (43°N–50°N, 0°W–15°W), Norway (60°N–70°N, 0°E–15°E), North Sea (50°N–60°N, 3°W–8°E) and western UK (50°N–60°N, 3°W–15°W). Each event is linked to a nearby cyclone, which is then tracked back in time for a maximum of 10 days and forward 1 day, as long as the maximum 10 m wind speeds exceed the tropical depression criterion (Beaufort 7; 13.9 m/s). The tracking algorithm consists of three steps. (1) First, an initial guess of the new position is made by extrapolating the 2 previous ones. (2) Next, the maximum relative vorticity (RV) in a surrounding 5° by 5° box is determined. If it corresponds to a lower MSLP than that of the initial guess, the new position is updated. (3) Finally, the centre location is determined by the MSLP minimum within a 2.5° radius of the latest estimate. This procedure is repeated every 3-hourly interval and uses MSLP and RV to track both tropical and extra-tropical cyclones. Especially TC remnants moving in the flow around a larger low pressure system can be followed back in time. Storms are detected only for the months August through November to exclude typical winter storms. To further focus on cyclones with a tropical origin, only those originating in the tropical Atlantic (0°N–38°N, 85°W–20°W) are selected. The northern boundary of this box is determined by the average northernmost expansion of the 26 °C isotherm over the studied period. The different regions used and the resulting sets of studied storms are given in Fig. S3 of the supplemental material.

3.4 Phase space analysis

To detect the presence of a warm seclusion and investigate the general life cycle of the selected storms, a phase space analysis is performed. A new method is proposed here that focuses on EPT and PV, attempting to make optimal use of the high horizontal resolution while minimising the limitations posed by the small number of pressure levels. To detect the presence of a warm core, the EPT of the centre (averaged over a 1° by 1° area) is compared to the minimum found within a 5° by 5° area south–east of the centre. As the studied storms generally move north-eastward, the latter region is indicative for a dry intrusion surrounding the centre of a warm seclusion storm. A conventional cold core cyclone will not show a large EPT difference as its warm sector is located away from the centre. Tropical cyclones generally have a symmetric warm core throughout most of the troposphere, represented by a high EPT difference while warm seclusions only do so at lower levels. Therefore calculations are done at 850 and 300 hPa, resulting into two parameters called DT_{850} and DT_{300}, respectively.

The strength of a TC is well indicated by its PV column while the diabatic heating in a warm seclusion results in a low-level PV maximum (which can be seen in Fig. 1f). The average PV of the storm core (again in a 1° by 1° area) is estimated at 775 hPa and at 400 hPa using the respective adjacent pressure levels to calculate the vertical temperature gradient. These parameters (PV_{775} and PV_{400}) are thus indicative for the intensity of a tropical cyclone as well as the presence of a warm seclusion.

The ETT of a TC can also be monitored well through Hart diagrams depicting the phase space analysis performed by Hart (2003), but data limitations impede its use here. Apart from the case study of Amy, data is only available at 5 pressure levels (850, 700, 500, 300 and 200 hPa) in addition to surface fields. This greatly limits the ability of performing a linear fit in the 900–600 hPa and 600–300 hPa vertical intervals. Hart diagrams are made using the 850–500 and 500–300 hPa layers and are shown in the supplemental material (Figs. S7 and S8).

3.5 Mean wind field

The wind field of the cyclones is investigated to detect the possible presence of a sting jet. For each storm, the timing

of the relative minimum in central MSLP is determined within 24 h of the moment when the 11 Beaufort wind selection criterion was met and referred to as 't$_0$'. This can also be done for other parameters such as maximum wind speed, PV or EPT difference. The average field of all storms can then be determined after interpolating each of the individual fields onto an equidistant grid to eliminate latitudinal dependencies.

3.6 Forcings during intensification

TCs moving out of the tropics carry a lot of moisture in both their core and through atmospheric rivers. For re-intensification, the presence of baroclinic instability is also of vital importance. Therefore, these three components are to be quantified by plain parameters. The core moisture can simply be represented by the vertically integrated specific humidity, summed over the inner 300 km region. The latitudinal dependency of grid box sizes is taken into account and the resulting parameter is called Q$_c$. The large scale flow of moisture towards the cyclone, possibly through atmospheric rivers is quantified using the integrated vapour transport (IVT, Lavers et al. 2013). It is calculated as the vertically integrated horizontal moisture flux in a box around the storm centre. This box spans 1500 km in the westerly, southerly and easterly direction and 750 km towards the north to incorporate most of the warm conveyor belt which may resemble an atmospheric river. With wind speeds of typically 30–40 m/s, this moisture has the potential to reach the core within about 12 h. Only moisture flowing towards the storm and outside of a 300 km radius surrounding the centre is considered and the sum over the entire box is taken (again after correcting for the latitudinal dependency of the zonal distance). This parameter, named IVT then represents the total amount of moisture being transported from the environment towards the storm. Finally, baroclinic instability can be quantified through the storm relative thickness asymmetry of the 850–500 hPa layer, in analogy to the parameter B in Hart (2003). In practice, the average thickness within the left and right semi-circle with a 750 km radius is determined relative to the storm motion and the difference is named Z$_d$. The three parameters are then calculated and given as a function of time in comparison to the cyclone intensity:

- IVT: summed integrated vapour transport over considered area (1500 km);
- Q$_c$: total amount of moisture in the core (300 km radius);
- Z$_d$: storm relative 850–500 hPa thickness asymmetry (750 km radius).

4 Results

4.1 Tracks and intensity

Consistent with the results in Haarsma et al. (2013), the number of Autumn storms originating in the tropical Atlantic increases significantly: from 15 in the present to 23 in near future and 37 in future simulations (Fig. 3). Additionally, the intensity of the storms increases, especially between the latter two periods as indicated by a lower minimum MSLP and higher wind speeds (Table 1). No such changes have been found in other, course resolution simulations (de Winter et al. 2013). Throughout the twentyfirst century, the genesis region of cyclones impacting Western Europe expands northward at first but then also eastward and westward. In addition to an eastward shift (Fig. S5), intense tropical cyclones forming in the Caribbean are also capable of reaching Europe even after a possible landfall in the US. Related to these changes is a shift in the affected region; while storms in the present climate usually peak in intensity west of the British Isles, they do so further northeast in the future. As a consequence, the North Sea region and Scandinavia will experience significantly more Autumn storms. Also the Bay of Biscay area will see a considerable increase in storminess.

A comparison was done between the acquired storm tracks from present climate simulations and those registered in the IBTrACS database (Knapp et al. 2010; Fig. S4). Using the same regions (Biscay, Norway, North Sea and UK), storms impacting Western Europe were selected for the 1981–2010 period. When considering only the storms exhibiting >50kt (10 min sustained) 10 m wind speeds (storm force) in one of the regions, a very similar pattern appears indicating that the model reproduces the studied storm tracks quite well. An interesting difference is the occurrence of cyclones originating in the Caribbean in the IBTrACS selection which is only simulated in the future. The observed SST used in the model is not necessarily representative for the entire 30-year period and therefore may not favour these storms but the results still indicate that their tracks become more likely in the future.

4.2 Final storm structure

The mean 850 hPa EPT field for all storms at their maximum intensity clearly shows the structure of a warm seclusion for both simulations (Fig. 4) and observations (Fig. S9). Similar to the development of Amy, a region of potentially warmer air is surrounded by the dry intrusion and almost cut off from the rest of the warm conveyor belt. In agreement with the Shapiro–Keyser conceptual model, the cyclones are consistently located near the left exit region
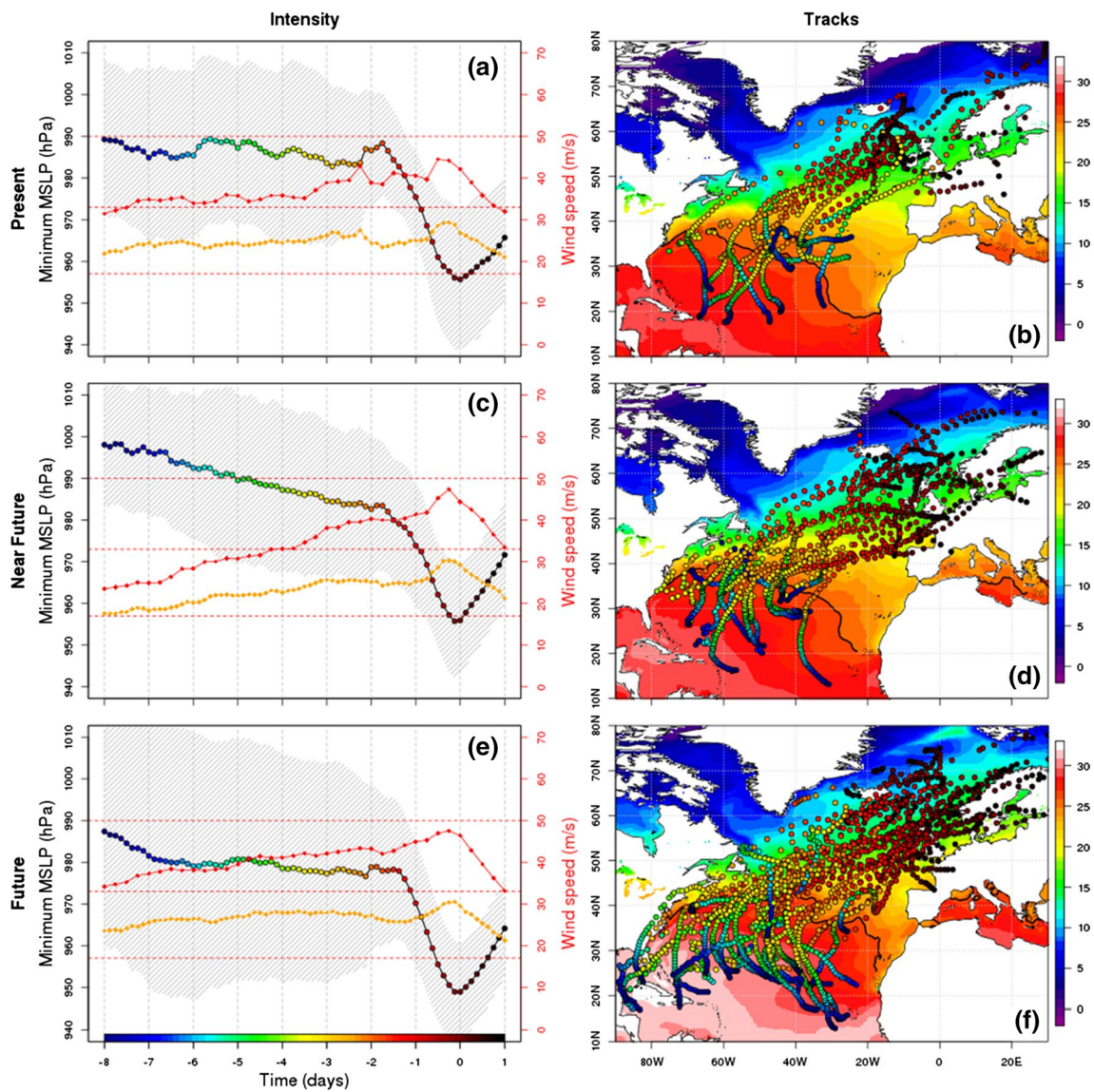
Fig. 3 Intensity and tracks for present (**a**, **b**), near future (**c**, **d**) and future (**e**, **f**) cyclones where the *left panels* contain minimum MSLP (*black edged circles*) and standard deviation (*hatching*), 10 m wind (*orange*) and 850 hPa wind (*red*). The *right panels* show the storm tracks and August–October mean SSTs (in °C) for the respective periods, the *thick black line* indicates the 26 °C isotherm. The *colour scale* of the *circles* indicates the time relative to t_0 in days and is the same everywhere, as indicated in (**e**)

Table 1 General information (central pressure, maximum 10 m wind speed and maximum 850 hPa EPT difference) about the number and intensity of post-tropical (PTC) and extratropical (ETC) storms in the three different periods (present, near future and future), all studied storms and rapidly intensifying cyclones (RI; >2 hPa/3 h)

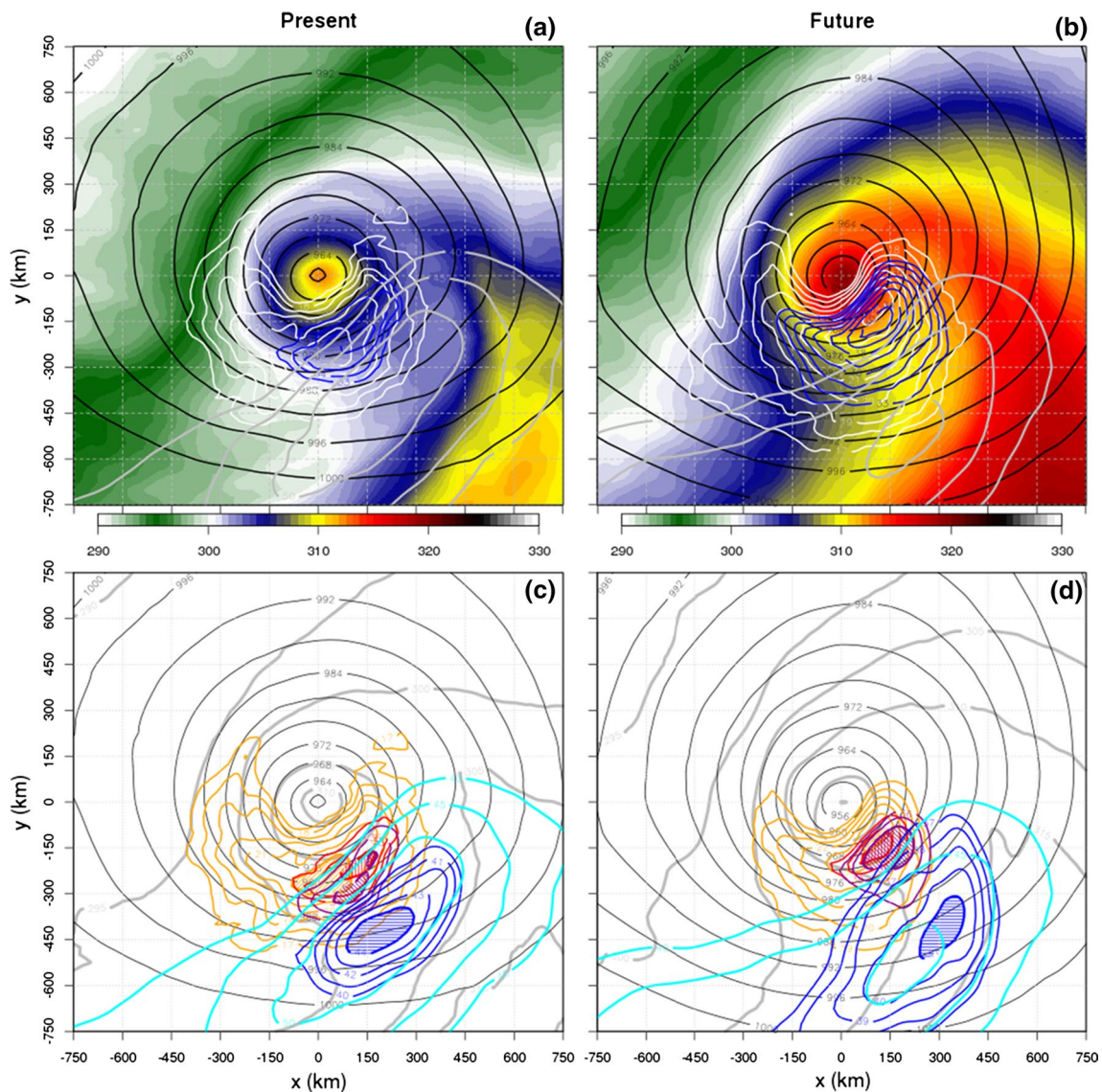|	Number	PTC	ETC	P_{min} (hPa)	$V_{10,max}$ (m/s)	$DT_{850,max}$ (K)
Present	15	10	5	955.2 ± 16.5	31.76 ± 2.63	17.28 ± 4.21
Near future	23	10	13	954.6 ± 13.2	32.61 ± 3.56	17.35 ± 5.81
Future	37	22	15	947.3 ± 11.7	33.46 ± 3.91	18.18 ± 5.57
All	75	44	33			
RI	50	22	28			

Fig. 4 Mean horizontal fields for all present (*left*) and future (*right*) storms, selected at the time of maximum 850 hPa wind. The *upper panels* show 850 hPa EPT (K) in *shading* and 10 m, 850 hPa and 300 hPa wind as *white*, *blue* and *grey contours*, respectively. In the *lower panels*, *coloured contours* depict wind speed at 10 m, 850, 700, 500 and 300 hPa (*orange*, *red*, *purple*, *blue* and *cyan*), EPT at 850 hPa is also drawn in *thick grey contours*. MSLP (hPa) is given everywhere by *black contours*

of a jet streak during the final stage of their evolution. A region with high 10 m wind speeds is expected to be south of the centre due to the generally eastward motion of the storms, which is also observed (Fig. 4a, b). The highest wind speeds, however, occur well to the east in a region that coincides with the end of the back bent front. Strong winds are also present at higher levels (Fig. 4c, d) and appear to be brought down from the jet stream. These results suggest that the occurrence of a sting jet is at least partially responsible for the observed high low-level wind speeds. Furthermore, all of the above features are much more pronounced for future storms. The latter are generally warmer and more moist, resulting in stronger fronts, more vertical

momentum exchange and consequently a better set-up for the occurrence of a sting jet. This phenomenon likely also occurs in present storms, but less frequently. Nevertheless, the vertical wind structure supports the development of a sting jet for both periods suggesting a stronger interaction between the different levels in the future.

4.3 Extratropical and post-tropical cyclones

The investigation of individual storms reveals that not all of them evolve into an actual TC during their early evolution. This partly explains the very large spread in central MSLP and the absence of an earlier MSLP minimum or

wind maximum that should be present if all storms were a mature TC at first (Fig. 3a, c, e). In the phase space analysis, core PV is determined as a measure for TC strength and can thus be used to distinguish mature TCs from other systems such as tropical depressions, subtropical storms or cold core extratropical cyclones. Only when the PV at both 775 and 400 hPa exceeds 3.5 potential vorticity units (PVU; 10^{-6} Km^2/kgs) at some point in the cyclone life cycle up to 24 h before t_0 (to exclude the final intensification), the cyclone is considered a mature TC. If not, the storm is said to be extratropical in nature, while it still originates in the tropics. The threshold was determined experimentally; the number of observed TCs showed only minor changes for values between 3 and 4 PVU. To avoid confusion on this matter, the former storms are referred to as post-tropical (as they undergo ETT) while the latter are called extratropical. It is important to note that the storms which are called extratropical here are not necessarily cold core systems as some may have a weak or shallow warm core.

The two subsets of storms now show a distinctly different pattern of evolution (Fig. 5). Post-tropical cyclones (PTCs) have an early peak in intensity, followed by a weakening during ETT and a subsequent re-intensification. Extra-tropical cyclones (ETCs), on the other hand, show no sign of a previous development apart from a rapid deepening in the last 24–48 h before t_0. The increased storminess in Europe in the near-future can be explained mainly by an increase of ETCs (13 vs. 5; Table 1). In fact, the number of PTCs is the same for the present and near future dataset. The increase in ETCs is probably related to a tightening of the meridional surface temperature gradient in their development region (Fig. S6). The latter is due to the northward expansion of the Atlantic warm pool while the cold Labrador Current remains in place (SST field in Fig. 3d). The area separating the regions of tropical and extratropical development consequently shrinks facilitating the transition of storms, especially weaker systems which are included among the ETCs. Although their frequency does not change, the intensity of PTCs increases in the near future, which is likely due to the increased SSTs. The future dataset mainly exhibits an increase in the number of PTCs. No further increase in the number of ETCs is simulated as the baroclinic zone shifts further northward thus ceasing the reduction of the transition area. These storms form deeper into the tropics and are well developed, allowing them to move further northward into a region that is not conducive for their development. As discussed in Haarsma et al. (2013), greater TC intensity and an eastward shift of the genesis region hence enable more storms to reach European coasts. A smaller transit area compared to that in the present climate still allows for an increased number of weak systems (considered to be ETCs) to cross.

4.4 Cyclone evolution

The phase space analyses of both EPT and PV show a very different life cycle for PTCs compared to ETCs (Fig. 6). As anticipated, TCs appear as deep warm core systems with strong PV structures several days back in time. After reaching a peak in intensity, they reach less favourable regions (usually higher wind shear and/or lower SSTs) and start weakening. At first, this is most pronounced in the upper part of the PV column, similar to what was observed for Amy (Fig. 1e). Eventually, all parameters indicate a degradation of the cyclone structure. During the last day before t_0, the system intensifies again in agreement with previous results (Fig. 5a, c, e). Most striking is the evolution of the EPT difference, which shows the development of a shallow warm core and suggests the presence of a warm seclusion. The associated low level PV anomaly is not as pronounced, but still suggested, and probably not well captured due to the limited vertical resolution. Finally, also the upper level EPT difference and core PV increase, which can be related to tropopause folding near the centre which increases both PV and potential temperature (Uccellini et al. 1985; see also Fig. 2c, d).

The life cycle of an extratropical system is very different; no general pattern of intensification is present before the last few days. These cyclones form as baroclinically unstable waves along the US East coast while drawing warm and moist air from the Gulf Stream region. While moving northward, they meet much colder air coming from the north resulting in large temperature contrasts and rapid intensification. Despite their distinct prehistory, both types of storms show a similar development during their final intensification with the formation of a shallow warm core. In consequence, at the final stage of their evolution both types of storms are almost indistinguishable.

In addition to the differences in storm life cycles between the storm subsets, there are also uneven changes towards the future climate. Tropical cyclones are becoming stronger, as both their warm core and PV column become more pronounced (Fig. 6). ETCs on the other hand show no major changes in evolution although there is a slight shift towards the development of a stronger low level PV core 2–4 days before t_0 (Fig. 6d, f). It seems that these are immature tropical cyclones that form in conditions only marginally favourable for their development and/or spend too little time over warm waters to evolve into mature TCs. The most notable fact remains the consistency in the development of a warm seclusion during the final intensification. This is probably related to the tropical origin of the storms resulting in large temperature and moisture gradients. ETCs generally form in the Western North-Atlantic which favours the development of LC1 type storms (Thorncroft et al. 1993; Schultz et al. 1998). PTCs re-intensify further
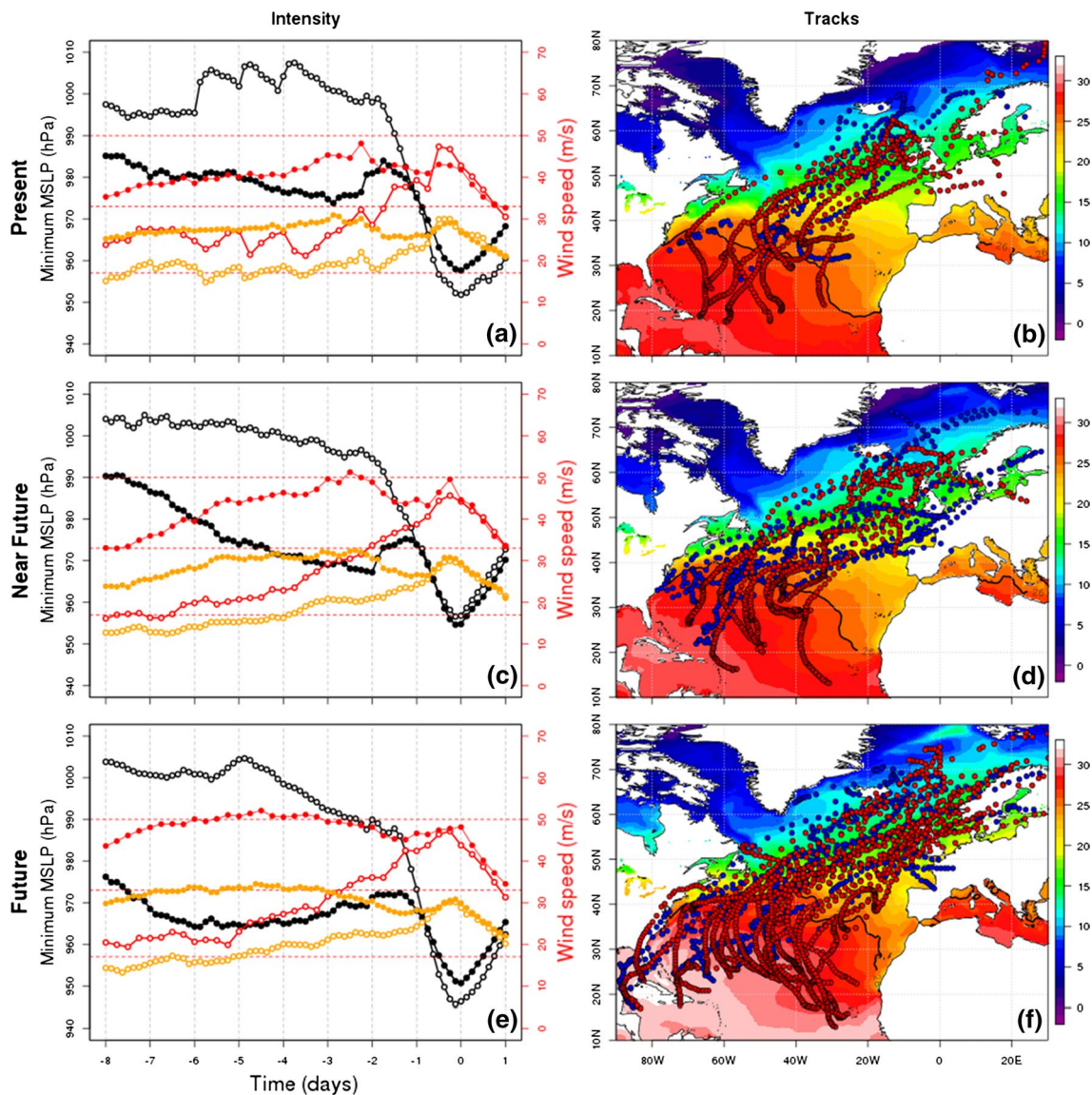
Fig. 5 Intensity (*left*) and tracks (*right*) for cyclones in the three different periods, similar to Fig. 3. In the *left panels* post-tropical cyclones are indicated by *filled circles* while open ones are used for extra-tropical systems. *Red markers* distinguish PTCs from ETCs (*blue*) in the *right panels*

east but have a strong influence on the upper level flow pattern (Orlanski and Sheldon 1995) in combination with the presence of a remnant warm core which alters the conditions for development.

4.5 Forcings and intensification

To analyse the intensification process, the roles of atmospheric rivers, baroclinic forcing and core moisture are estimated. The general evolution is quite similar for the different periods (Fig. 7) with a phase of intensification in the last 24–48 h that coincides with a maximum in baroclinic forcing (Z_d). The amount of moisture that is transported into the storm as indicated by IVT generally does not vary much on average during the final development, while the part that resides in the core steadily decreases as the system moves into a colder environment. ETCs in the near future and future have high initial IVT values, suggesting that most of them are indeed immature tropical cyclones (such as tropical depressions or subtropical storms). For individual cases there is often a drop in IVT, reaching a minimum before (re-)intensification starts. At this point, the atmospheric river regains strength and gradually decays again when the storm weakens and/or its surroundings become colder. On average, this effect is not clearly visible due to the different timing and the occasionally strongly dropping
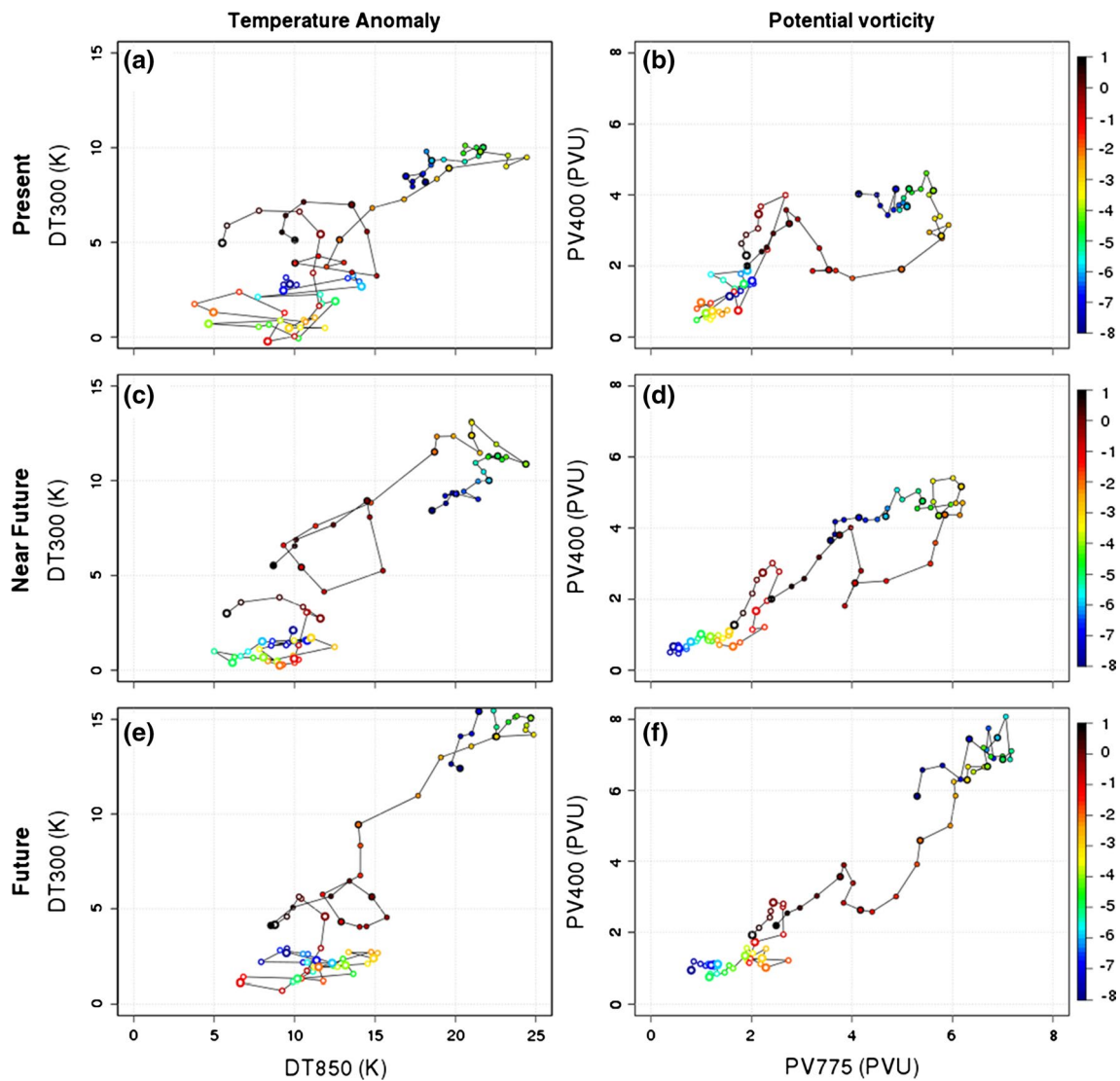
Fig. 6 Phase space analysis of PTCs (*filled*) and ETCs (*open*) for present (**a**, **b**), near future (**c**, **d**) and future (**e**, **f**). *Thick edges* indicate 24 h intervals and *colour* marks the time relative to t_0 (in days)

IVT in storms that lose their atmospheric river. When separating PTCs from ETCs, a slight increase in IVT during the early intensification can be seen, occurring earlier for the latter. Considering the total IVT and core moisture over the studied period, both increase strongly in future cyclones. This again indicates that storms will become warmer, carry more moisture and be more intense. A slight decrease in baroclinic forcing is seen for near future cyclones. This may be related to a decrease in the large scale temperature gradient but also to the fact that weaker systems are able to reach the mid latitudes and re-intensify.

The main contributions to the intensification can be demonstrated by comparing the total pressure drop with the summed forcing over the corresponding 6-hourly time steps. This is done for the intensification period, defined by

the time during which the central MSLP deepens within the last 48 h leading to t_0. The respective pressure drop is then simply the difference between the begin and end value of the selected period. For all parameters the last step is excluded, as is the second to last one for the IVT, since they are indicative for the forcing that results in the consecutive intensification. In general, the pressure drop correlates well with both the total IVT and baroclinic forcing (Fig. 8a, b). When taking the normalised sum of both, the correlation is even higher, indicating that both forcings are most effective when occurring simultaneously. There is a large overlap between different periods and storm types, in correspondence to the large variance seen in Fig. 7. The main differences are that ETCs on average have a larger pressure drop as well as a stronger baroclinic forcing and that they show better correlations
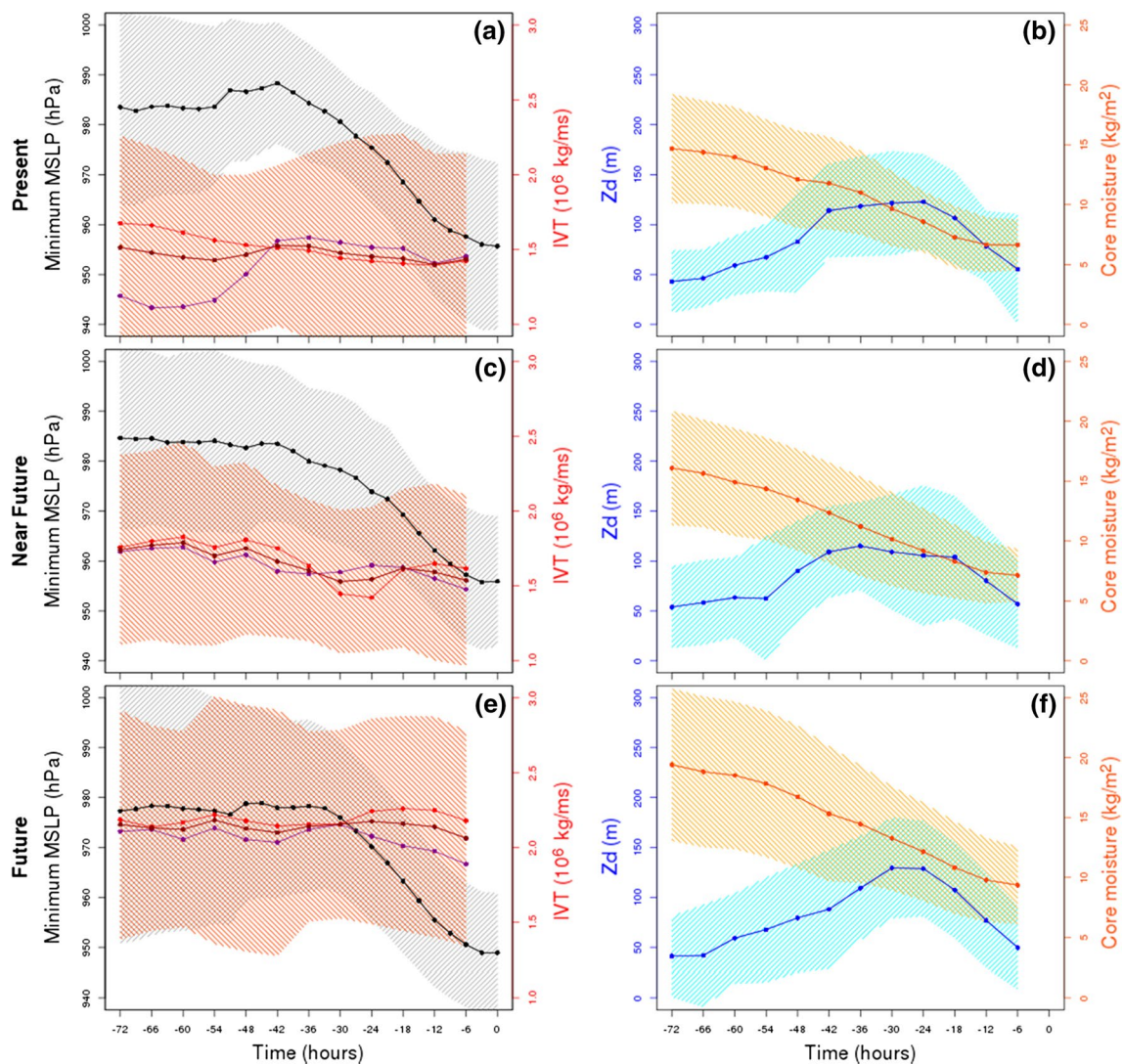
Fig. 7 Mean minimum MSLP (*black*) and total IVT (*red*) on the left and thickness asymmetry (Z_d, *blue*) and core moisture (*orange*) on the right side for all present, near future and future storms. Standard deviations for each value are indicated by the *hatched regions* and for the IVT the average result for PTCs and ETCs is shown separately in *light red* and *purple*, respectively

with the amount of core moisture. PTCs are characterised by slightly lower correlations for IVT, but show no link at all to the amount of core moisture. This indicates that the moisture provided by an atmospheric river is more important than that residing in a warm core remnant for the final intensification.

An overview of all the parameters for the different subsets can be found in Table 2 and their associated correlations are shown in Table 3. The latter contains an additional subset of rapidly intensifying cyclones, exhibiting an average pressure drop of at least 2 hPa/3 h over the intensification period. For these storms, higher correlations are found mainly for PTCs, in particular the IVT. Especially PTCs in the near future are characterised by bad correlations overall. This is probably caused by the presence of hybrid storms that do not complete their ETT and consequently exhibit little to no re-intensification.

These storms are characterised by an asymmetric or frontal structure while still having a warm core, such as Hurricane Sandy of 2012. Amy also has some hybrid properties, showing a long ETT and only little decrease in strength but still a considerable re-intensification. Some of the future cyclones are also hybrids but the large increase in PTCs lowers their relative contribution to the average result. The presence of hybrid storms is further suggested by individual Hart diagrams (Figs. S7 and S8) and a principal component analysis, presented in the supplemental material (Table S2).

In summary, both atmospheric rivers and baroclinic instability are important for the intensification of the studied storms. The intensification is initialised by baroclinic forcing after which the atmospheric river often strengthens and provides a positive feedback loop by feeding the storm
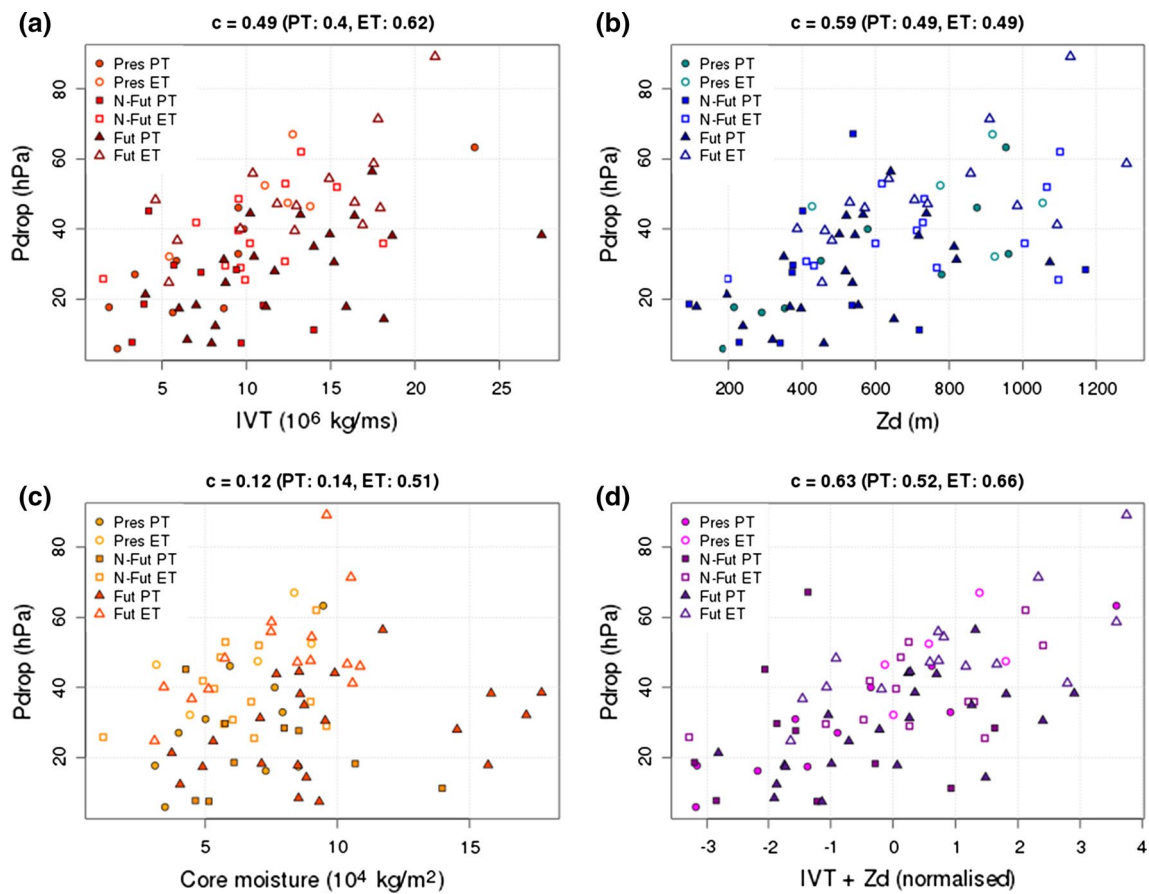
Fig. 8 Scatter plot comparing the pressure drop during intensification with total IVT (**a**), 850–500 hPa thickness asymmetry (Z_d; **b**), core moisture (**c**) and the sum of normalised IVT and Z_d (**d**) for all storms over a maximum of 48 h before t_0. The different periods as well as post-tropical (PT) and extratropical (ET) cyclones are distinguished. Above each panel is the according correlation of the respective parameter with the pressure drop along with those for separate subsets of PT and ET systems

Table 2 Summed forcings during the intensification period (max 48 h) and the associated drop in central MSLP: moisture flux (IVT), baroclinic forcing (Z_d) and core moisture (Q_c) for simulated present, near future and future cyclones and distinguishing post-tropical (PT) from extratropical (ET) systems

	Subset	IVT (10^6kg/ms)	Z_d (m)	Q_c (10^4kg/m^2)	Pdrop (hPa)
Present	All	9.05	649.28	6.29	36.21
	PT	8.03	564.05	6.23	29.75
	ET	11.11	819.74	6.39	49.12
Near Future	All	9.19	619.05	6.68	33.52
	PT	7.38	477.26	7.08	26.13
	ET	10.58	728.12	6.37	39.20
Future	All	12.66	617.70	8.87	36.97
	PT	12.37	528.60	9.68	28.18
	ET	13.09	748.39	7.68	49.85

A similar result taking a fixed 48 h period is given in table S1

with warm and moist air. Although a correlation does not say anything about causality, the fact that often an atmospheric river is already present before the intensification suggests that they are also of great importance. Moreover, the large increase in total IVT means that more tropical air in atmospheric rivers will influence the future European climate accompanied by a higher potential for floods.

5 Conclusions

This analysis of EC-Earth simulations shows that in a warmer future climate, Western Europe will see larger impacts from severe Autumn storms. Not only their frequency will increase, but also their intensity and the area they affect. The structure of most storms resembles that

Table 3 Correlations of the different total forcings (moisture flux, baroclinic forcing, core moisture and the normalised sum of the first 2) with their associated pressure drop over the intensification period (max 48 h)

	Subset	IVT (10^6kg/ms)	Z_d (m)	Q_c (10^4kg/m^2)	IVT + Z_d
Present	All	**0.82**	**0.73**	0.50	**0.88**
	PT	**0.86**	**0.82**	**0.55**	**0.92**
	ET	0.70	0.04	0.67	0.66
Near Future	All	0.19	0.41	-0.21	0.33
	PT	-0.36	0.16	-0.43	-0.11
	ET	0.44	0.46	0.27	**0.53**
Future	All	**0.50**	**0.65**	0.13	**0.68**
	PT	**0.52**	**0.48**	0.33	**0.60**
	ET	**0.67**	**0.64**	**0.55**	**0.74**
All	All	**0.47**	**0.59**	0.10	**0.61**
	PT	**0.39**	**0.49**	0.20	**0.51**
	ET	**0.58**	**0.48**	**0.45**	**0.64**
All RI	All	**0.56**	**0.57**	0.27	**0.65**
	PT	**0.60**	**0.47**	0.36	**0.64**
	ET	**0.62**	**0.56**	**0.48**	**0.70**

Font styles indicate significance levels (<90, 90, **95** and **99 %**) using Student's *t* test of correlation. Results for present, near future and future storms are considered, as well as all and all rapidly intensifying systems (RI; >2 hPa/3 h). The correlations slightly differ from those shown in Fig. 8 as the parameters where normalised first for each period using the according mean and variance but the result is very similar

of a warm seclusion cyclone in both simulated and reanalysis data. This is probably related to the conditions in their genesis region and the tropical air they carry. As observation that was not anticipated is the different prehistory of storms. The assumption was that all Autumn storms originating in the tropics are TCs that undergo ETT and subsequently re-intensify as ETCs. Especially for the near future, a large increase is found in storms that do not evolve into a mature TC. In fact, these storms are more likely to reach Europe because the transit region between the (sub)tropics and the baroclinic zone shrinks. In the latter part of the twenty-first century, the expansion and eastward shift of the hurricane genesis region will result into more storms curving towards Europe and impacting a larger region. Warmer SSTs generally lead to the formation of stronger TCs but also more powerful warm seclusion storms. A summary of the main changes in tracks, origin and impacted region between the present, near future and future simulations is presented in Fig. 9.

The mean 850 hPa EPT clearly depicts the warm seclusion as a region of potentially warmer air which is separated from the warm conveyor belt. Their location close to a jet streak and the alignment of horizontal wind at different levels allows for the development of a sting jet. Although the results for all periods suggest the presence of a sting jet in at least part of the storms, this feature is most pronounced in future cyclones.

Both baroclinic instability and atmospheric rivers are important for the (re-)intensification of the considered storms. The former is most important for extra-tropical development while the latter provides heat and moisture that enhances the latent heat release in a newly forming warm core as well as in the warm conveyor belt, thus speeding up the intensification. In addition, atmospheric rivers are often already present beforehand, suggesting that they play an important role in the process. Core moisture does not seem to play an important role as most transitioning cyclones lose their warm core to reform one with high EPT air from the warm conveyor belt. For ETCs there is a higher correlation with core moisture but this is because they form a warm core that carries more moisture as they intensify. Baroclinic instability does not decrease significantly for future studied storms, as a tightening EPT gradient (Fig. S6) and more latent heat release counteract the effects of a northward shift of the polar jet stream. The inflow of moisture increases greatly, resulting in more intense storms that carry more moisture.

In general, it can be said that tropical air will have a greater impact on the future European weather through more severe Autumn storms. It is important to note that this study is based on the results of only one future climate scenario and a single model which is forced by SST estimates. It is therefore hard to assess uncertainties and to validate the results, which should be clarified by future work in high resolution modelling.
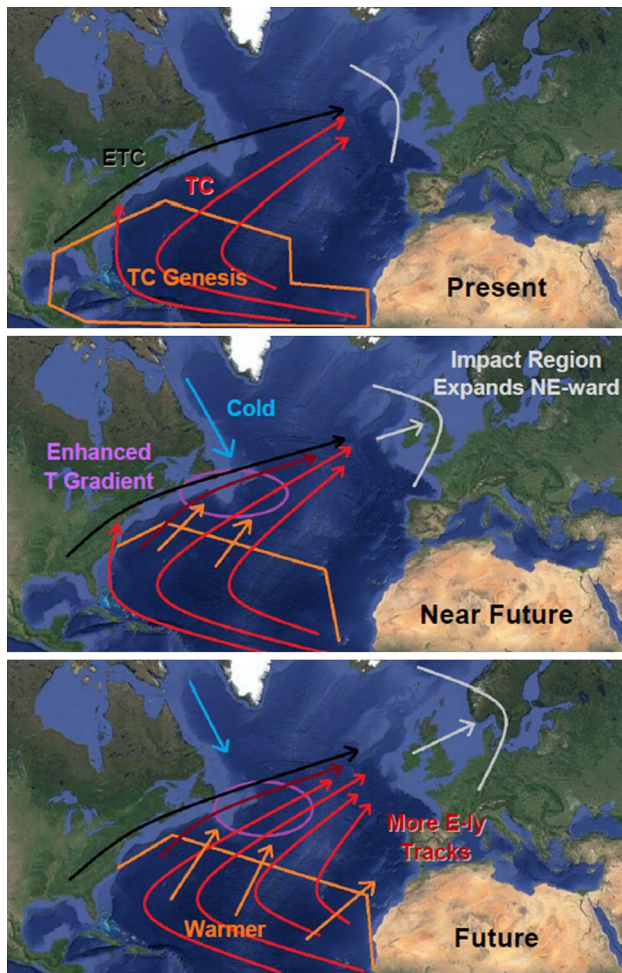
Fig. 9 Summary of the changes in the tracks of severe Autumn storms impacting Western Europe in the present, near future and future climate. The TC genesis region is indicated in *orange*, storm tracks in *red* (TCs) and *black/dark red* (ETCs). The *grey line* indicates the extent of the impact of such storms in Europe

References

Agusti-Panareda A, Thorncroft CD, Craig GC, Gray SL (2004) The extratropical transition of hurricane Irene: a potential-vorticity perspective. Q J Roy Meteorol Soc 130:1047–1074

Baker L (2009) Sting jets in severe northern European wind storms. Weather 64:143–148

Bjerknes J (1919) On the structure of moving cyclones. Geofys Publ 1:1–8

Bjerknes J, Solberg H (1922) Life cycle of cyclones and the polar front theory of atmospheric circulation. Geofys Publ 3:1–18

Browning KA (2004) The sting at the end of the tail: damaging winds associated with extratropical cyclones. Q J Roy Meteorol Soc 130:375–399

Davies HC, Schär C, Wernli H (1991) The palette of fronts and cyclones within a baroclinic wave environment. J Atmos Sci 48:1666–1689

de Winter RC, Sterl A, Ruessink BG (2013) Wind extremes in the north sea basin under climate change: an ensemble study of 12 CMIP5 GCMs. J Geophys Res Atmos 118:1601–1612

Dorland C, Tol RSJ, Palutikof P (1999) Vulnerability of the Netherlands and Northwest Europe to storm damage under climate change. Clim Change 43:513–535

Galarneau TJ, Davis CA, Shapiro MA (2013) Intensification of Hurricane Sandy through extratropical warm core seclusion. Mon Weather Rev 141:4296–4321

Haarsma RJ, Hazeleger W, Severijns C, de Vries H, Sterl A, Bintanja R, van Oldenborgh GJ, Van den Brink HW (2013) More hurricanes to hit western Europe due to global warming. Geophys Res Lett 40:1–6

Hart RE (2003) A cyclone phase space derived from thermal wind and thermal asymmetry. Mon Weather Rev 131:585–616

Hazeleger W, Severijns C, Semmler T, Stefanescu S, Yang S, Wang X, Wyser K, Dutra E, Bintanja R, van den Hurk B, van Noije T, Selten F, Sterl A (2010) EC-Earth: a seamless earth-prediction approach in action. B Am Meteorol Soc 91:1357–1363

Hoskins BJ (1990) Theory of extratropical cyclones. In: Newton CW, Holopainen EO (eds) Extratropical cyclones, the Erik Palmén memorial volume. Am Meteorol Soc, Boston, pp 64–80

Hoskins BJ, Simmons AJ, Andrews DG (1977) Energy dispersion in a barotropic atmosphere. Q J Roy Meteorol Soc 103:553–567

Jones SC, Harr PA, Abraham J, Bosart LF, Bowyer PJ, Evans JL, Hanley DE, Hanstrum BN, Hart RE, Lalaurette F, Sinclair MR, Smith RK, Thorncroft C (2003) The extratropical transition of tropical cyclones: forecast challenges, current understanding, and future directions. Weather Forecast 18:1024–1092

Knapp KR, Kruk MC, Levinson DH, Diamond HJ, Neumann CJ (2010) The international best track archive for climate stewardship (IBTrACS): unifying tropical cyclone best track data. B Am Meteorol Soc 91:363–376

Lavers DA, Allan RP, Villarini G, Lloyd-Hughes B, Brayshaw DJ, Wade AJ (2013) Future changes in atmospheric rivers and their implications for winter flooding in Britain. Environ Res Lett 8:034010

Maue RN (2010) Warm seclusion extratropical cyclones. Florida State University

Orlanski I, Sheldon JP (1995) Stages in the energetics of baroclinic systems. Tellus A 47:605–628

Rogelj J, Meinshausen M, Knutti R (2012) Global warming under old and new scenarios using IPCC climate sensitivity range estimates. Nat Clim Change 2:248–253

Schultz DM, Keyser D, Bosart LF (1998) The effect of large-scale flow on low-level frontal structure and evolution in midlatitude cyclones. Mon Weather Rev 126:1767–1791

Schwierz C, Köllner-Heck P, Mutter EZ, Bresch DN, Vidale P, Wild M, Schär C (2009) Modelling European winter storm losses in current and future climate. Clim Change 101:485–514

Shapiro MA, Keyser D (1990) Fronts, jet streams, and the tropopause. In: Newton CW, Holopainen EO (eds) Extratropical Cyclones, the Erik Palmén memorial volume. Am Meteorol Soc, Boston, pp 167–191

Sterl A, Severijns C, Dijkstra H, Hazeleger W, van Oldenborgh GJ, van den Broeke M, Burgers G, van den Hurk B, van Leeuwen PJ, van Velthoven P (2008) When can we expect extremely high surface temperatures? Geophys Res Lett 35:14

Thorncroft CD, Hoskins BJ, McIntyre ME (1993) Two paradigms of baroclinic-wave life-cycle behaviour. Q J Roy Meteorol Soc 119:17–55

Uccellini LW, Keyser D, Brill KF, Wash CH (1985) The president's day cyclone of 18–19 February 1979: influence of upstream

trough amplification and associated tropopause folding on rapid cyclogenesis. Mon Weather Rev 113:962–988

van Delden A (1989) On the deepening and filling of balanced cyclones by diabatic heating. Meteorol Atmos Phys 41:127–145

van den Hurk BJJM, Viterbo P, Beljaars ACM and Betts AK (2000) A.K.: offline validation of the ERA40 surface scheme; ECMWF TechMemo 295. http://www.ecmwf.int/publications/library/ecpublications/pdf/tm/001-300/tm295.pdf

van Vuuren DP et al (2011) The representative concentration pathways: an overview. Clim Change 109:5–31

Wernli H, Dirren S, Liniger MA, Zillig M (2002) Dynamical aspects of the life cycle of the winter storm 'Lothar' (24–26 December 1999). Q J Roy Meteorol Soc 128:405–429

Zhu Y, Newell RE (1998) A Proposed Algorithm for Moisture Fluxes from Atmospheric Rivers. Mon Weather Rev 126:725